

Reliable Localization Using Set-Valued Nonlinear Filters

Giuseppe Calafiore

Abstract—In this paper, we propose a novel methodology for reliable localization of an autonomous mobile robot navigating in an unstructured environment using noisy absolute measurements from its exteroceptive sensors. A new deterministic filtering technique is introduced, which is based on the recursive computation of a bounding set that is guaranteed to contain the true state of the system, despite process and observation noise, and taking into explicit consideration uncertainties due to the linearization error. The proposed set-valued nonlinear filter relies on a two-step prediction–correction structure, with each step requiring the solution of a particular convex optimization problem. The method is illustrated by simulation on a localization problem for a nonholonomic rover, and it is compared with the standard extended Kalman filter approach.

Index Terms—Bounded uncertainty, linear matrix inequalities, mobile robot localization, nonlinear filters.

I. INTRODUCTION

THE accurate determination of position and orientation of a mobile robot with respect to a fixed reference frame (absolute localization) is a key requirement for autonomous navigation in unstructured environments. For this reason, the localization problem has been extensively studied in the robotics literature (see for instance [4], [12], [14], and [20], and the references therein). The mainstream approach for robot localization is Bayesian estimation, which is based on stochastic assumptions about the process and measurement errors, and is aimed to constructing the posterior density of the current robot state, conditioned on all available measurements. In particular, when the process and measurement error processes are assumed Gaussian, the Bayesian approach results in the classical extended Kalman filtering (EKF) framework (see [2], [11], and [14]). However, in robotics applications, the distribution of the sensor and process noise is generally multimodal and imprecisely known, and the nonlinearities of the system may seriously degrade the EKF performance. These limitations have been recognized in the literature, and several schemes have been proposed to overcome them. Notably, an adaptive EKF approach for on-line estimation of the noise statistics have been proposed in [12] and [18], and joint Bayesian hypothesis testing and Kalman filtering have been proposed in [19]. A probabilistic confidence set approach has been presented in

[16], which is optimal over a certain class of noise distributions, and a Monte Carlo approach, where the noise density is represented by means of a set of randomly drawn samples, is proposed in [7]. The effects of the linearization errors on the EKF are studied in [10].

In this paper, we depart from the Bayesian approach, and propose a new methodology for reliable localization which requires no assumption on the noise statistics; the only assumption is that process and measurement errors are bounded in magnitude by some known quantity. We call this localization method “reliable” since the algorithm provides a bounding ellipsoidal set that is *guaranteed* to contain the true state of the system, despite process and measurement disturbances and linearization errors. Reliable localization is of course critical in mobile applications, as well as in manipulation tasks, since failure to capture the true pose within the confidence set may result in a collision or task failure. The solution is computed recursively and it is based on a two-step prediction-correction structure, in analogy with the EKF. Each step of the algorithm requires the solution of a semidefinite optimization problem (SDP), which is a special convex optimization problem that may be solved numerically with great efficiency (see [5], [9], and [21]).

Set-valued filters have already been studied for the linear case (see, e.g., [3] and [15]). In the classic literature on this topic (referred to also as deterministic, ellipsoidal, or set-membership filtering), a bounding set for the state of a linear system is computed recursively, starting from deterministic assumptions on the noise affecting the system, which is assumed to be an unknown-but-bounded (UBB) sequence, instead of a stochastic sequence. A similar approach based on interval analysis is also studied in [13]. The use of semidefinite optimization in deterministic robust filtering problems has been pioneered in [8].

The paper is organized as follows. In Section II, the notation is set and the class of systems of interest is introduced. In Section III, the two-step set-valued filter for reliable localization is presented (main results in Theorem 1 and Theorem 2), and the algorithm for the filter recursion is given. Section IV presents a simulated numerical example of application to localization of a nonholonomic rover, and a comparisons with the EKF localization method are made. The conclusion is drawn in Section V.

II. PROBLEM STATEMENT AND NOTATION

The robot localization approach presented in this paper may be viewed as direct application of a general technique for robust set-valued nonlinear filtering. This technique is treated in generality in the present and in the following section. Implementation issues and details of application to robot localization are deferred to Section IV.

Manuscript received October 30, 2002; revised March 25, 2004. This work was supported by FIRB and PRIN “MATRIX” funds from the Italian Ministry of University and Research. This paper was recommended by Associate Editor W. Martin.

The author is with the Dipartimento di Automatica e Informatica, Politecnico di Torino, Torino 24-10129, Italy (e-mail: giuseppe.calafiore@polito.it).

Digital Object Identifier 10.1109/TSMCA.2005.843383

The sampled dynamics of the robot may be described by means of a discrete-time nonlinear system of the form

$$x_{k+1} = f(x_k, u_k) + B_k w_k \quad (1)$$

where $x_k \in \mathbb{R}^n$, $u_k \in \mathbb{R}^{n_u}$ denote the state and input vectors at time k , respectively, $w_k \in \mathbb{R}^{n_w}$ is a noise vector, and standard regularity assumptions are required on the the function $f(\cdot, \cdot)$. The noise affecting the system is assumed to be an UBB sequence, i.e., $\|w_k\| \leq 1$, for all k .¹ This noise description is often more realistic than a stochastic description in many applications. We do not assume knowledge of a particular probability distribution on the noise, but rather assume deterministic bounds on its amplitude. These bounds are obtained by physical considerations on the plant and sensors and actuators models.

Associated to the system equations, there is a nonlinear measurements map

$$y_k = h(x_k, u_k) + D v_k \quad (2)$$

where $y_k \in \mathbb{R}^{n_y}$ is the output measurement vector, and $v_k \in \mathbb{R}^{n_v}$ is a bounded noise vector, $\|v_k\| \leq 1$. In the context of robot localization, the measurement equation represents absolute measurements from the robot exteroceptive sensors.

Based on an initial set-valued estimate of the state and on the noisy measurements, our goal is to recursively compute set-valued estimates for the state of the system, in the form of ellipsoids of minimal size (in the sense that the sum of the squared semiaxes lengths is minimized) that guarantee to contain the “true” state of the system, for any possible value of the uncertainty and linearization error. This robust filtering procedure has its natural applications in strong tracking for nonlinear systems, and in localization problems.

The set estimate will be computed in two steps, in a way similar to the EKF: a prediction step, and a measurement update step. The main differences with respect to the EKF framework are that 1) we are no longer in a stochastic noise setting and 2) we explicitly impose a robustness condition against linearization errors. The resulting equations are more complicated than the Riccati recursions, but can still be solved very efficiently using recently developed interior-point semidefinite programming (SDP) algorithms [9], [21].

In the following, we shall use the notation $\mathcal{E}(x, E)$ to denote the ellipsoid $\{\xi : \xi = x + Ez, \text{ for some } z : \|z\| \leq 1\}$, having center x and shape matrix E . When $P \doteq EE^T \succ 0$ (the sign \succ means “positive definite”) an alternative representation is $\{\xi : (\xi - x)^T P^{-1} (\xi - x) \leq 1\}$. The “size” of the ellipsoid is measured by means of the sum of squared semiaxes lengths, which is given by $\text{Tr}P$, where Tr is the trace function. The symbol $\|X\|$ denotes the Euclidean norm of X , if X is a vector, and the spectral (maximum singular value) norm of X , if X is a matrix.

III. ROBUST SET-VALUED NONLINEAR FILTER

A. Set-Valued State Prediction

In the first step, we assume to have a previous set-valued estimate of the state, in the form of a bounding ellipsoid $\mathcal{E}_k(\hat{x}_k, E_k)$

¹The condition $\|w_k\| \leq 1$ amounts to considering *spherical* noise. Generic *ellipsoidal* noise can be treated in our framework in a straightforward way, by suitably scaling the noise-influence matrix B_k .

with center \hat{x}_k and shape matrix E_k , i.e., we assume that at the time instant k

$$x_k = \hat{x}_k + E_k z, \quad \text{for some } z \text{ such that } \|z\| \leq 1. \quad (3)$$

The state equations (1) can be linearized about the central estimate \hat{x}_k as

$$x_{k+1} = (A_k + L_a \Delta_a)(x_k - \hat{x}_k) + B_k w_k + \tilde{u}_k \quad (4)$$

where $\tilde{u}_k = f(\hat{x}_k, u_k)$ and

$$A_k = \left. \frac{\partial f(x, u)}{\partial x} \right|_{x=\hat{x}_k; u=u_k}$$

where L_a is a problem-dependent scaling matrix, and $\Delta_a \in \mathbb{R}^{n, n}$ is some unknown matrix, such that $\|\Delta_a\| \leq 1$. The uncertainty term Δ_a has a double interpretation: together with the scaling L_a it takes into account uncertainty in the model matrix A_k due to neglected higher order terms in the Taylor series expansion of the original nonlinear model (1). A rigorous justification of the validity of this representation for the linearization error is given in Appendix C. Alternatively, it may be viewed as a “robustification” term, introduced to take into account generic model inaccuracies in the matrix A_k . If one wants instead to neglect the effects of linearization errors and/or model uncertainties, L_a should be set to zero.

The robust prediction step is now aimed at determining a new ellipsoid $\mathcal{E}_{k+1|k}(\hat{x}_{k+1|k}, E_{k+1|k})$, which guarantees to contain the state x_{k+1} , for any allowable value of the noise and linearization error. In formulas, we want to compute $P_{k+1|k}$, $\hat{x}_{k+1|k}$, such that the condition

$$(x_{k+1} - \hat{x}_{k+1|k})^T P_{k+1|k}^{-1} (x_{k+1} - \hat{x}_{k+1|k}) \leq 1 \quad (5)$$

holds for any $\|z\| \leq 1$, $\|w_k\| \leq 1$, and $\|\Delta_a\| \leq 1$. The matrix $E_{k+1|k}$ is then computed from $P_{k+1|k}$ by means of Cholesky factorization. The result for robust prediction is given in the following theorem.

Theorem 1: If (3) and (4) hold, then a predicted bounding ellipsoid $\mathcal{E}_{k+1|k}$ for the state at time $k + 1$ can be computed by solving the following semidefinite program in the variables $P_{k+1|k} \succ 0$, $\tau_z, \tau_w, \tau_a > 0$, $\hat{x}_{k+1|k}$

$$\begin{aligned} & \text{minimize } \text{Tr}P_{k+1|k} \\ & \text{subject to } \tau_z, \tau_w, \tau_a \succ 0 \\ & \begin{bmatrix} P_{k+1|k} & \Phi(\hat{x}_{k+1|k}) \\ \Phi^T(\hat{x}_{k+1|k}) & \Omega(\tau_z, \tau_w, \tau_a) \end{bmatrix} \succ 0 \end{aligned} \quad (6)$$

where

$$\begin{aligned} \Phi(\hat{x}_{k+1|k}) & \doteq [\tilde{u}_k - \hat{x}_{k+1|k} \quad A_k E_k \quad B_k \quad L_a] \\ \Omega(\tau_z, \tau_w, \tau_a) & \doteq \text{diag}(1 - \tau_z - \tau_w, \tau_z I \\ & \quad -\tau_a E_k^T E_k, \tau_w I, \tau_a I). \end{aligned} \quad (7)$$

The proof of this theorem is reported in Appendix A. \square

We remark that computing the optimal solution of the optimization problem in Theorem 1 requires essentially $O(n^3)$ operations, which is thus comparable with the numerical complexity of the prediction step of a standard EKF. The $O(n^3)$ complexity figure is obtained by first reformulating the problem in a suitable decoupled form, and then solving the decoupled problem via an interior-point barrier method for convex programming. Explicit details on this operation are found in [6].

B. Measurement Update

At the measurement step, we are given the predicted ellipsoid $\mathcal{E}_{k+1|k}$ for the state x_{k+1} , i.e.,

$$x_{k+1} = \hat{x}_{k+1|k} + E_{k+1|k}z, \quad \text{for some } z \text{ such that } \|z\| \leq 1 \quad (8)$$

where $E_{k+1|k}E_{k+1|k}^T = P_{k+1|k}$, and we want to update this information with the one coming from the current measurement y_{k+1} . To this end, we linearize the output equations (2) about the current estimate $\hat{x}_{k+1|k}$, obtaining

$$y_{k+1} = (C_{k+1} + L_c \Delta_c)(x_{k+1} - \hat{x}_{k+1|k}) + Dv_{k+1} + \tilde{h}_{k+1} \quad (9)$$

where $\Delta_c \in \mathbb{R}^{n_y, n}$ is some matrix such that $\|\Delta_c\| \leq 1$ which, together with the problem-dependent scaling matrix L_c , takes into account the remainder due to the linearization error and/or the uncertainty in the measurement matrix C_{k+1} (see also the discussion in Section III-A and Appendix C), and

$$C_{k+1} = \left. \frac{\partial h(x, u)}{\partial x} \right|_{x=\hat{x}_{k+1|k}; u=u_{k+1}}$$

$$\tilde{h}_{k+1} = h(\hat{x}_{k+1|k}, u_{k+1}).$$

The updated ellipsoid $\mathcal{E}_{k+1}(\hat{x}_{k+1}, E_{k+1})$ that is guaranteed to contain the state x_{k+1} , should satisfy the condition

$$(x_{k+1} - \hat{x}_{k+1})^T P_{k+1}^{-1} (x_{k+1} - \hat{x}_{k+1}) \leq 1 \quad (10)$$

whenever the equality

$$y_{k+1} = (C_{k+1} + L_c \Delta_c)E_{k+1|k}z + Dv_k + \tilde{h}_{k+1} \quad (11)$$

holds for some $\|z\| \leq 1$, $\|v_k\| \leq 1$, and $\|\Delta_c\| \leq 1$. The result for the computation of the updated bounding ellipsoid is given in the following theorem.

Theorem 2: Assume that (8) and (9) hold. Let

$$\Phi_y \doteq [\tilde{h}_{k+1} - y_{k+1} \quad C_{k+1}E_{k+1|k} \quad D \quad L_c] \quad (12)$$

and let Ψ be an orthogonal complement of Φ_y , i.e., a matrix of full-rank, such that $\Phi_y \Psi = 0$. Then, the updated bounding ellipsoid for the state x_{k+1} is given by the solution of the following SDP in the variables $P_{k+1} \succ 0$, $\tau_z, \tau_v, \tau_c \succ 0$, \hat{x}_{k+1}

$$\begin{aligned} & \text{minimize } \text{Tr} P_{k+1} \\ & \text{subject to } \tau_z, \tau_v, \tau_c \succ 0 \\ & \begin{bmatrix} P_{k+1} & \Phi_m(\hat{x}_{k+1})\Psi \\ \Psi^T \Phi_m^T(\hat{x}_{k+1}) & \Psi^T \Omega_m(\tau_z, \tau_v, \tau_c)\Psi \end{bmatrix} \succ 0 \end{aligned} \quad (13)$$

where

$$\begin{aligned} \Phi_m(\hat{x}_{k+1}) & \doteq [\hat{x}_{k+1|k} - \hat{x}_{k+1} \quad E_{k+1|k} \quad 0 \quad 0] \\ \Omega_m(\tau_z, \tau_v, \tau_c) & \doteq \text{diag}(1 - \tau_z - \tau_v, \tau_z I \\ & \quad - \tau_c E_{k+1|k}^T E_{k+1|k}, \tau_v I, \tau_c I). \end{aligned} \quad (14)$$

The proof of this theorem is reported in Appendix B. \square

Computing the optimal solution of the optimization problem in Theorem 2 requires essentially $O(n^3)$ operations (see [6] for details on how this complexity figure is obtained).

Remark: The measurement update result presented in the above theorem is useful also for sensor fault detection. Geometrically, in Theorem 2, we compute an ellipsoid of minimal size that covers the intersection of the predicted ellipsoid $\mathcal{E}_{k+1|k}$ with the set of states compatible with the measurement equation (11). Therefore, if the numerical code that solves (13) determines a P_{k+1} whose trace is (numerically) zero, then it means that the intersection is void, and the collected measurement y_{k+1} is not compatible either with the output uncertainty model, or with the prediction model. This situation may happen when the actual process or measurement errors exceed the assumed bounds. In this case, the datum can be removed as an outlier (measure failure), and the predicted ellipsoid $\mathcal{E}_{k+1|k}$ is carried over for the next step.

C. Algorithm for Robust Filter Recursion

The procedure for the recursive computation of the state-bounding ellipsoids is summarized below. In the algorithm, the notation \hat{x} is used to denote the state estimate at the current time k , and \hat{x}_+ is used to denote the predicted forward state estimate $\hat{x}_{k+1|k}$. An analogous notation is used for the other quantities of interest.

Init.: Given an initial bounding ellipsoid $\mathcal{E}_0(\hat{x}_0, E_0)$, and the current value of input u_0 , select a time horizon T_h , and set $k=0$. Let $\hat{x} \leftarrow x_0$, $u \leftarrow u_0$, $E \leftarrow E_0$.

State lin.: Get linearized model of state equations in the form (4).

Prediction: Solve SDP (6) to obtain P_+ and \hat{x}_+ . The matrix $E_+ \doteq E_{k+1|k}$ is then obtained from the Cholesky factorization of P_+ : $P_+ = E_+ E_+^T$.

Meas. update: Set $k \leftarrow k+1$;

1. If measurement is not available, then set $\hat{x} \leftarrow \hat{x}_+$, $E \leftarrow E_+$ and goto Loop; else collect measurement y , and get linearized model of output equations in the form (9).

2. Solve SDP (13) to determine the new optimal P and \hat{x} , and determine new E by Cholesky factorization of P .

3. If $\text{Tr}P$ is lower than a prespecified threshold, then warn "Measurement not compatible with uncertainty model", and set $\hat{x} \leftarrow \hat{x}_+$, $E \leftarrow E_+$.

Loop: If $k == T_h$ then Exit, Else Goto **State lin.**

In Section IV, we present an application of this filtering algorithm to a mobile robot localization problem, and compare the performances of the robust filter with the ones obtained by the

EKF. For clarity of exposition, a basic implementation of the EKF is reported in the next section.

1) *EKF Recursion*: Using the same notation as in the previous section, we denote with \hat{x}_k^{EKF} the EKF state estimate at the current time k , and with \hat{x}_+^{EKF} the predicted forward EKF state estimate $\hat{x}_{k+1|k}^{\text{EKF}}$. Let Q_k be the process-error covariance, and R be the measurement-error covariance. The current filter covariance matrix is denoted as P^{EKF} , and the prediction covariance as P_+^{EKF} . An analogous notation is used for the other quantities of interest. The EKF recursion is as follows:

Init.: Given an initial state estimate \hat{x}_0^{EKF} , initial covariance P_0^{EKF} , and the current value of input u_0 , select a time horizon T_h , and set $k = 0$. Let $\hat{x}^{\text{EKF}} \leftarrow x_0$, $u \leftarrow u_0$.

State lin.: Get linearized model of state equations in the form (4).

Prediction:

$$\begin{aligned}\hat{x}_+^{\text{EKF}} &= f(\hat{x}^{\text{EKF}}, u) \\ P_+^{\text{EKF}} &= A_k P^{\text{EKF}} A_k^T + Q_k\end{aligned}$$

Meas. update: Set $k \leftarrow k + 1$;

1. If measurement is not available, then set $\hat{x}^{\text{EKF}} \leftarrow \hat{x}_+^{\text{EKF}}$, $P^{\text{EKF}} \leftarrow P_+^{\text{EKF}}$ and goto Loop; else collect measurement y , and get linearized model of output equations in the form (9).
- 2.

$$\begin{aligned}S &= C P_+^{\text{EKF}} C^T + R; \\ K &= P_+^{\text{EKF}} C^T S^{-1}; \\ \hat{x}^{\text{EKF}} &= \hat{x}_+^{\text{EKF}} + K (y - h(\hat{x}_+^{\text{EKF}}, u)); \\ P^{\text{EKF}} &= P_+^{\text{EKF}} - K S K^T.\end{aligned}$$

Loop: If $k == T_h$ then Exit, Else Goto **State lin.**

2) *Comparing Deterministic and Stochastic Filter Results*: The robust deterministic filter of Section III-C and the stochastic filter of Section III-C1 require different inputs and provide different outputs. Here, we briefly discuss how to consistently compare these results. The robust filter requires an initial estimate in the form of an ellipsoid \mathcal{E}_0 with center \hat{x}_0 and shape matrix P_0 , and returns bounding ellipsoids \mathcal{E}_k for the state. The stochastic filter requires instead an initial estimate in the form of an expected value \hat{x}_0^{EKF} and covariance matrix P_0^{EKF} , and returns expected values \hat{x}_k^{EKF} and covariances P_k^{EKF} for the state. From the covariance information, however, we can extract a (probabilistic) confidence ellipsoid for the state, that can be compared with the ellipsoid provided by the robust filter. To this end, consider the ellipsoid

$$\mathcal{E}_k^{\text{EKF}}(r) \doteq \left\{ x \in \mathbb{R}^n : (x - \hat{x}_k^{\text{EKF}})^T \times (r^2 P_k^{\text{EKF}})^{-1} (x - \hat{x}_k^{\text{EKF}}) \leq 1 \right\}.$$

Now, if x is an n -dimensional random vector distributed according to the normal (Gaussian) distribution $N(\hat{x}_k^{\text{EKF}}, P_k^{\text{EKF}})$, with mean \hat{x}_k^{EKF} and covariance matrix P_k^{EKF} , then the random

variable $z = (x - \hat{x}_k^{\text{EKF}})^T (P_k^{\text{EKF}})^{-1} (x - \hat{x}_k^{\text{EKF}})$ has the χ^2 density with n degrees of freedom, i.e., the probability density function of z is as follows (see for instance Theorem 3.3.3 of [1]):

$$f_z(\zeta) = \frac{1}{2^{\frac{n}{2}} \Gamma(\frac{n}{2})} e^{-\frac{\zeta}{2}} \zeta^{\frac{n}{2}-1}.$$

Therefore, the probability of the event $\{x \in \mathcal{E}_k^{\text{EKF}}(r)\}$ is given by the integral of $f_z(\zeta)$, from zero to r^2 . In other words, $\text{Prob}\{x \in \mathcal{E}_k^{\text{EKF}}(r)\} = \mathcal{X}^2(r^2, n)$, where $\mathcal{X}^2(r^2, n)$ denotes the χ^2 cumulative distribution function with n degrees of freedom. This function, as well as its inverse, is tabulated in standard numerical tables, and is also available in numerical software packages such as Matlab. Hence, for given probability level $\gamma \in (0, 1)$, we can determine the radius $r(\gamma)$ such that the ellipsoid $\mathcal{E}_k^{\text{EKF}}(r(\gamma))$ contains x with probability γ ; $\mathcal{E}_k^{\text{EKF}}(r(\gamma))$ thus represents a γ -confidence ellipsoid for the state of the system. A plot of the dependence of the scaling factor r on γ is depicted in Fig. 1. From this plot, we notice for instance that if the state dimension is $n = 3$, then, multiplying the EKF filter covariance P_k^{EKF} by a scaling factor r^2 , with $r = 3.5$, we obtain a confidence ellipsoid that contains the state with probability greater than 99%. This ‘‘confidence’’ should, however, be interpreted with care, since it holds only as long as the linearity and Gaussian hypotheses on the noises hold. This is indeed one of the main motivations of the present paper: when nonlinearities are present and/or the noise distribution is not Gaussian, then the confidence regions determined via the EKF approach can be very misleading (see also the results of the examples Section IV).

IV. APPLICATION: RELIABLE LOCALIZATION OF A NONHOLONOMIC ROBOT

In this section, we illustrate the use of the robust filtering algorithm on a two-dimensional localization problem for a unicycle robot equipped with sonar sensors, and compare reliability and performance of our technique with those obtained using an EKF.

Consider the mobile robot depicted in Fig. 2. Let x_1, x_2 be the coordinates of the main axis midpoint with respect to a fixed reference frame, and let $x_3 = \theta$ be the angle between the robot forward axis and the x_1 direction. The kinematic (odometric) model of the unicycle is described by the following:

$$\begin{aligned}\dot{x}_1(t) &= \nu(t) \cos x_3(t) \\ \dot{x}_2(t) &= \nu(t) \sin x_3(t) \\ \dot{x}_3(t) &= \omega(t)\end{aligned}$$

where $\nu(t)$ and $\omega(t)$ denote, respectively, the linear and angular velocities of the robot. By means of the change of coordinates (chained form [11], [17])

$$\begin{aligned}\xi_1 &= -x_3 \\ \xi_2 &= x_1 \cos x_3 + x_2 \sin x_3 \\ \xi_3 &= x_2 \cos x_3 - x_1 \sin x_3\end{aligned}$$

and assuming zero-order hold on $\omega(t)$ and $\nu(t)$, the above system can be integrated exactly, and then discretized with sample time T and expressed in linear form as

$$\xi_{k+1} = A_k \xi_k + u_k + B_k w_k$$

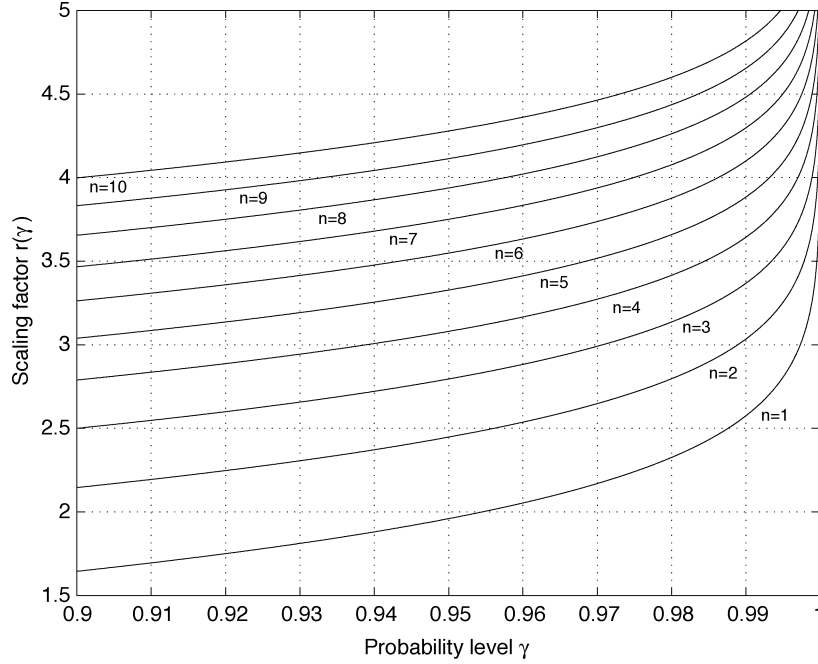


Fig. 1. Scaling factor $r(\gamma)$ for determination of the γ -confidence ellipsoid for various values of the state dimension n .

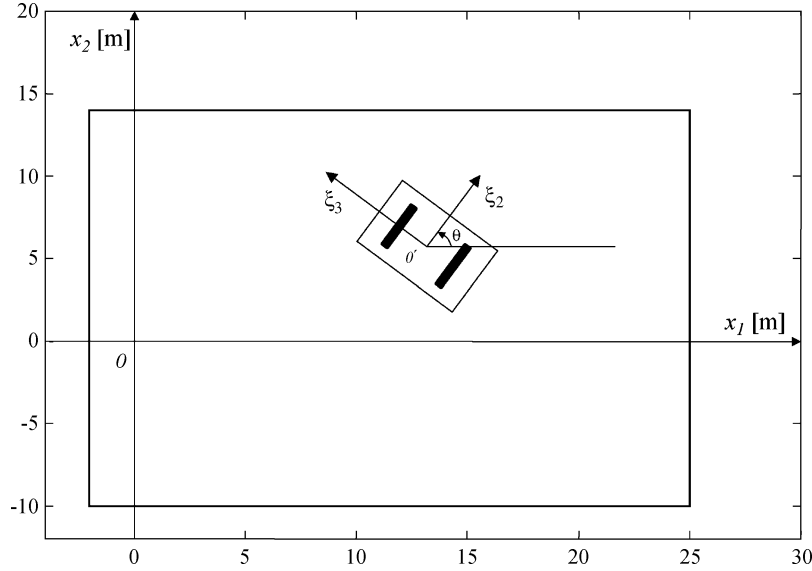


Fig. 2. Mobile robot in an indoor environment.

where

$$A_k = \begin{bmatrix} 1 & 0 & 0 \\ 0 & \cos(T\omega_k) & \sin(T\omega_k) \\ 0 & -\sin(T\omega_k) & \cos(T\omega_k) \end{bmatrix}$$

$$u_k = \begin{bmatrix} -T\omega_k \\ \frac{\sin(T\omega_k)\nu_k}{\omega_k} \\ \frac{(\cos(T\omega_k)-1)\nu_k}{\omega_k} \end{bmatrix}$$

and w_k , $\|w_k\| \leq 1$ is UBB noise that accounts for model inaccuracies (e.g., wheel slippage, misalignments, etc.). Further details and justification for the use of the chained-form description may be found in [11].

The robot is equipped with five sonar sensors, ideally placed at the robot center, with orientation of $-\pi/2, -\pi/4, 0, \pi/4, \pi/2$

with respect to the robot forward axis. The sonar measurement map is nonlinear, and depends on the environment description. The environment is depicted in Fig. 2, and is constituted by four vertical planes, whose normals form the angles $\pi, \pi/2, 0, -\pi/2$ with the x_1 direction, and whose distances from the origin are 2, 14, 25, 10 m, respectively. Each sonar has a beamwidth $\delta = 80^\circ$; expressions for the range measurements in relation to the environment description, and the selection of the valid sonar readings have been implemented as detailed in [12]. Echoes and crosstalk interferences have been neglected in the simulation.

The noise influence matrix is chosen of the form $B_k = B\nu_k/\nu_{\max}$, where ν_{\max} is the maximum nominal value of the imposed linear velocity, and $B = \text{diag}(0.014, 0.014, 0.014)$. This accounts for the fact that process uncertainty is higher when the robot is moving faster. The sonar range reading error

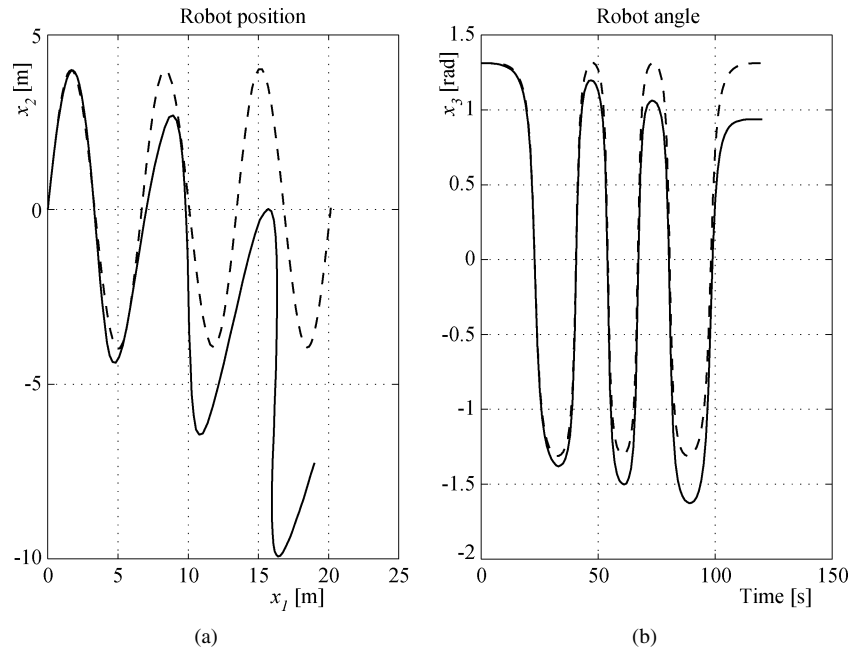


Fig. 3. Second simulation. (a) Nominal (dashed line) and actual (solid line) robot trajectory in the $x_1 - x_2$ plane. (b) Nominal (dashed line) and actual (solid line) robot angle $x_3 = \theta$.

is assumed to have maximum amplitude $D = 0.05I$ m. The scaling matrix L_a is zero, since system dynamics are linear (no linearization error), while L_c is also set to zero, thus deliberately neglecting output linearization error, in order to fairly compare the set-valued filter results with the EKF.

For comparison purposes, we performed numerical simulations in two different situations. In the first simulation, the process and measurement noises have been generated as Gaussian random sequences with covariance matrices $Q_k = (B_k/3.5)^2$ and $R = (D/3.5)^2$, respectively.² The data provided to the robust filter are the error bound information B_k , D , while the data provided to the Extended Kalman filter are the noise covariances Q_k and R . It is clear that this situation is advantageous for the EKF, since its Gaussian noise hypotheses are exactly satisfied.

In the second simulation, the process and measurement noises have been generated as uniform random sequences, satisfying the amplitude bounds described by the matrices B_k and D , and were further polarized in sign. As before, the data provided to the EKF are the covariance matrices $Q_k = (B_k/3.5)^2$ and $R = (D/3.5)^2$ (but the noise is no longer Gaussian), while the data provided to the robust filter are the error bounds described by B_k and D .

In both simulations, the imposed nominal trajectory is a sinusoidal path, and the system evolves in open loop, therefore, process errors are accumulated. The time horizon is $T_h = 120$ s, the sampling interval is $T = 1$ s, and it is assumed that measurement information is available every $T_{\text{upd}} = 5$ s. At the sampling instants when no measurement is available, both filters propa-

gate forward their predicted estimate. The nominal and actual trajectory for the second simulation is depicted in Fig. 3.

In the simulations, the ellipsoids of confidence computed by the filters are projected onto the first two components of the state, to obtain ellipsoids of confidence for the robot position in the $x_1 - x_2$ plane, and onto the third component of the state, to obtain confidence intervals for the robot orientation θ . For the EKF, the ellipsoids of confidence (to more than 99% probability) were computed multiplying the filter covariance by the scaling factor 3.5^2 , as discussed in Section III-C2.

In the first simulation, the robust filter yielded a root-mean-squared (rms) localization error of 0.0128 m, while the EKF yielded a slightly higher rms error of 0.0143 m. Moreover, the EKF confidence ellipsoid failed to contain the true state of the system 28% of the times. Thus, even in the (unrealistic) case of purely Gaussian noise, the EKF performance may degrade, due to nonlinearities in the system.

The results of the second simulation are displayed in Figs. 4 and 5. Fig. 4 shows the localization sets computed by the robust filter for the position and attitude of the robot.

Fig. 5 shows a particular of the second simulation, where the 99% ellipsoids of confidence computed by means of the EKF are added to the plot. The typical situation at a given point of the robot trajectory is that EKF gives deceptive confidence information, and fails to contain the true state of the system; the robust filter gives instead a reliable confidence set, that *always* guarantees containment of the true state. Notice that, in this simulation, the 99% EKF confidence set *never* contained the actual robot state. This confirms that the confidence results obtained from the EKF should be interpreted with great care whenever the actual operating conditions depart from the ideal assumptions under which the filter has been designed.

The rms localization error resulted to be 0.1 m for the EKF, and 0.082 m for the robust filter, therefore the robust filter

²The 3.5 factor has been used since a Gaussian random variable with standard deviation $D/3.5$ has more than 99% probability of being bounded in amplitude by D , therefore 3.5 is used as a “conversion factor” from bounded distribution to Gaussian distributions, and vice-versa. See also the discussion at the end of Section III-C2.

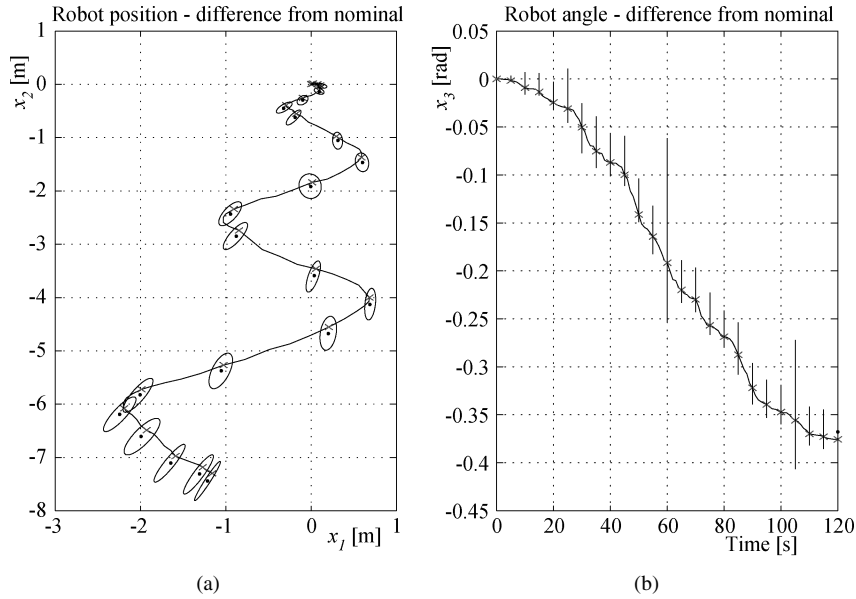


Fig. 4. Second simulation. All data is plotted relative to the nominal trajectory (i.e., differences of position and angles with respect to the nominal trajectory are plotted). (a) Actual robot positions (crosses) and their ellipsoids of confidence computed by the set-valued filter. Dots represent the center of the confidence ellipsoids. (b) Actual robot attitude (crosses) and their intervals of confidence computed by the set-valued filter. Dots represent the center of the confidence intervals.

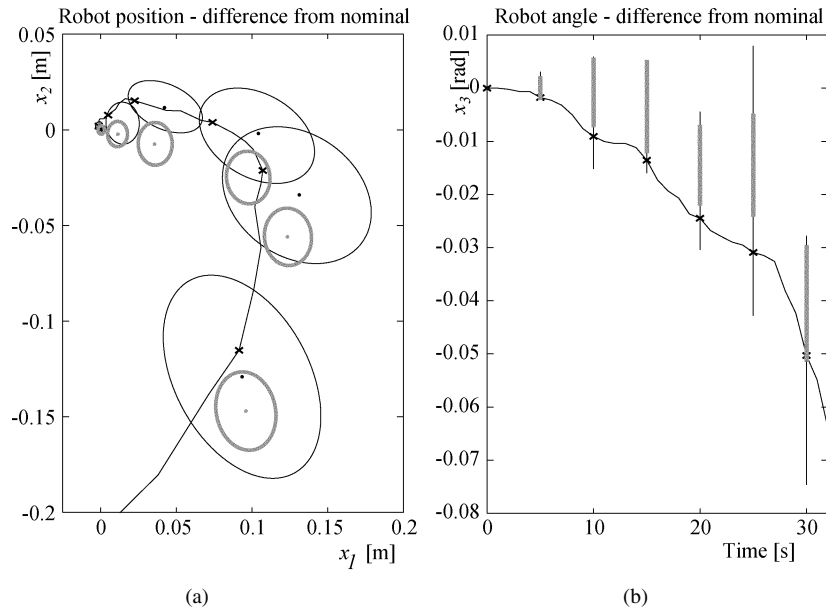


Fig. 5. Second simulation, particular. All data is plotted relative to the nominal trajectory (i.e., differences of position and angles with respect to the nominal trajectory are plotted). (a) Actual robot positions (crosses) and their ellipsoids of confidence computed: 1) by the set-valued filter (light line) and 2) by means of the EKF (bold line). (b) Actual robot attitude (crosses) and their intervals of confidence computed by: 1) the set-valued filter (light line) and 2) by means of the EKF (bold line).

yielded again superior performance also in terms of average localization errors, i.e., the centers of the localization ellipsoids are closer to the true robot position than the centers computed by the EKF.

V. CONCLUSION

This paper presented a novel methodology for reliable localization, based on a robust recursive nonlinear filtering algorithm which relies on deterministic assumptions on the noise and uncertainties affecting the system. This approach removes two

long-standing drawbacks of the classical stochastic approach to localization, namely the need of an accurate model of the noise statistics, and the effects of linearization errors. The filter provides set-valued estimates of the system state, that give guaranteed information on the location of the state, despite the noise and the linearization errors. This reliable knowledge may play an important role in robotic tasks such as navigation through narrow passageways, or in manipulation tasks, where accurate pose estimation is needed. The filter also provides a systematic way to check the model assumptions and therefore to pinpoint observations affected by gross errors and/or system failures.

On the simulated experiments, the robust filter provided superior performance with respect to the EKF approach. In practical situations, where the system is subject to polarization, misalignments, and offsets, that cannot be effectively modeled as Gaussian noise. The latter approach tends to provide erroneously small confidence sets around its estimates.

APPENDIX

A. Proof of Theorem 1

First, we write the prediction error $x_{k+1} - \hat{x}_{k+1|k}$, taking into account (3) and (4)

$$x_{k+1} - \hat{x}_{k+1|k} = \tilde{u}_k - \hat{x}_{k+1|k} + A_k E_k z + B w_k + L_a \Delta_a E_k z.$$

Defining

$$p_a = \Delta_a q_a \quad \|\Delta_a\| \leq 1. \quad (15)$$

with $q_a = E_k z$, we can restate the prediction error in the alternate form

$$\begin{aligned} x_{k+1} - \hat{x}_{k+1|k} &= \tilde{u}_k - \hat{x}_{k+1|k} + A_k E_k z + B w_k + L_a p_a \\ &= \Phi(\hat{x}_{k+1|k}) \xi. \end{aligned}$$

where we defined

$$\begin{aligned} \xi^T &\doteq [1 \quad z^T \quad w_k^T \quad p_a^T] \\ \Phi(\hat{x}_{k+1|k}) &\doteq [\tilde{u}_k - \hat{x}_{k+1|k} \quad A_k E_k \quad B \quad L_a]. \end{aligned}$$

We now notice that the conditions (15) are equivalent to

$$p_a^T p_a - q_a^T q_a \leq 0.$$

Therefore, we have that (5) holds for any $\|z\| \leq 1$, $\|w_k\| \leq 1$, $\|\Delta_a\| \leq 1$ if and only if the condition

$$\xi^T \Phi^T(\hat{x}_{k+1|k}) P_{k+1|k}^{-1} \Phi(\hat{x}_{k+1|k}) \xi \leq 1$$

holds whenever the following inequalities are satisfied

$$\begin{aligned} \xi^T \text{diag}(-1, I, 0, 0) \xi &\leq 0 \\ \xi^T \text{diag}(-1, 0, I, 0) \xi &\leq 0 \\ \xi^T \text{diag}(0, -E_k^T E_k, 0, I) \xi &\leq 0. \end{aligned}$$

A sufficient condition for the previous to hold is given by the so-called \mathcal{S} -procedure, [5]: there exist positive scalars τ_z , τ_w , τ_a such that

$$\begin{aligned} \xi^T &\left(\Phi^T(\hat{x}_{k+1|k}) P_{k+1|k}^{-1} \Phi(\hat{x}_{k+1|k}) - \text{diag}(1, 0, 0, 0) \right. \\ &\quad - \tau_z \text{diag}(-1, I, 0, 0) - \tau_w \text{diag}(-1, 0, I, 0) \\ &\quad \left. - \tau_a \text{diag}(0, -E_k^T E_k, 0, I) \right) \xi < 0. \end{aligned}$$

In turn, the above condition is true for all ξ if and only if

$$\Omega(\tau_z, \tau_w, \tau_a) - \Phi^T(\hat{x}_{k+1|k}) P_{k+1|k}^{-1} \Phi(\hat{x}_{k+1|k}) \succ 0$$

where Ω is defined as in (7). The statement of the theorem then follows by straightforward application of the Schur complement rule to the above matrix inequality. \square

B. Proof of Theorem 2

We outline the proof, which is similar to the one of Theorem 1. Define

$$p_c = \Delta_c q_c \quad \|\Delta_c\| \leq 1 \quad (16)$$

with $q_c = E_{k+1|k} z$. Then, the expression of the filtering error, using the information from the prediction step in (8), results in

$$x_{k+1} - \hat{x}_{k+1} = \Phi_m(\hat{x}_{k+1}) \xi$$

where Φ_m is defined as in (14), and $\xi^T \doteq [1 \quad z^T \quad v_k^T \quad p_c^T]$. Similarly, the measurement equation (11) may be expressed as

$$\Phi_y \xi = 0 \quad (17)$$

where Φ_y is defined as in (12). This means that all vectors ξ which are compatible with (17) must be of the form $\Psi \eta$, for some vector η , being Ψ an orthogonal complement of Φ_y .

Noticing now that the conditions (16) are equivalent to

$$p_c^T p_c - q_c^T q_c \leq 0$$

we have that (10) holds for any $\|z\| \leq 1$, $\|v_k\| \leq 1$, $\|\Delta_c\| \leq 1$, and it is compatible with the output equation, if and only if the condition

$$\eta^T \Psi^T \Phi_m^T(\hat{x}_{k+1}) P_{k+1}^{-1} \Phi_m(\hat{x}_{k+1}) \Psi \eta \leq 1$$

holds whenever the following inequalities are satisfied

$$\begin{aligned} \eta^T \Psi^T \text{diag}(-1, I, 0, 0) \Psi \eta &\leq 0 \\ \eta^T \Psi^T \text{diag}(-1, 0, I, 0) \Psi \eta &\leq 0 \\ \eta^T \Psi^T \text{diag}\left(0, -E_{k+1|k}^T E_{k+1|k}, 0, I\right) \Psi \eta &\leq 0. \end{aligned}$$

Using the \mathcal{S} -procedure, as we did in the proof of Theorem 1, we have that a sufficient condition for the previous to hold is the existence of positive scalars τ_z , τ_v , τ_c , such that

$$\Psi^T \left(\Omega_m(\tau_z, \tau_v, \tau_c) - \Phi_m^T(\hat{x}_{k+1}) P_{k+1}^{-1} \Phi_m(\hat{x}_{k+1}) \right) \Psi \succ 0$$

where Ω_m is defined as in (14). The statement of the theorem then follows by straightforward application of the Schur complement rule to the above matrix inequality. \square

C. Linearization With Bounded Error

We here provide a rigorous justification for the use of the introduced representation of the linearization error.

Consider a function $f : \mathbb{R}^n \rightarrow \mathbb{R}^n$, let $\hat{x} \in \mathbb{R}^n$ be a given point, and denote with f_i the i th component of f , which is assumed to be twice continuously differentiable. From classical analysis, the first-order Taylor series expansion of f about \hat{x} may be expressed as

$$f(x) = f(\hat{x}) + A(x - \hat{x}) + \mathcal{R}(x - \hat{x}) \quad (18)$$

where we defined

$$A = \left. \frac{\partial f(x)}{\partial x} \right|_{x=\hat{x}}$$

$$\mathcal{R} = \frac{1}{2} \begin{bmatrix} (x - \hat{x})^T F_1(x(\theta_1)) \\ \vdots \\ (x - \hat{x})^T F_n(x(\theta_n)) \end{bmatrix}$$

$$[F_i(x(\theta_i))]_{r,c} = \left. \frac{\partial^2 f_i(x)}{\partial x_r \partial x_c} \right|_{x=x(\theta_i)}$$

where $[X]_{r,c}$ denotes the element in the row r and column c of the matrix X , and $x(\theta_i) = \theta_i \hat{x} + (1 - \theta_i)x$, for some $\theta_i \in [0, 1]$. The last term in (18) represents the remainder of the series expansion, and involves the Hessian matrices F_i of the i th element of f , computed at unknown points on the line segment between x and \hat{x} .

We now elaborate on the expression of the remainder, for the case when x is bounded in an ellipsoid \mathcal{E} of center \hat{x} and shape matrix E , that is $x = \hat{x} + Ez$, for some $z \in \mathbb{R}^n$ with $\|z\| \leq 1$. Since the Hessians are assumed continuous, their norm reaches an extremum on the bounded domain \mathcal{E} , therefore it follows that there exist constants m_1, \dots, m_n such that, for $i = 1, \dots, n$, $\|F_i(x)\| \leq m_i$, for all $x \in \mathcal{E}$. In practical situations, the constants m_i may be determined by numerical computation. Since $x_k - \hat{x}_k = Ez$, with $\|z\| \leq 1$, then $\|(x_k - \hat{x}_k)^T F_i(x(\theta_i))\| \leq \|E\| m_i$ and, therefore, there exist vectors ξ_i , $\|\xi_i\| \leq 1$ such that $\|(x_k - \hat{x}_k)^T F_i(x(\theta_i))\| = \|E\| m_i \xi_i^T$. In other words, there exist a matrix $\mathcal{X}^T = [\xi_1 \ \dots \ \xi_n]$ with columns in the set $\{\|\xi_i\| \leq 1, \forall i\}$, such that $\mathcal{R} = 1/2 \|E\| \text{diag}(m_1, \dots, m_n) \mathcal{X}$. On the other hand, it may be easily verified that for any matrix \mathcal{X} in the above set, we have $\|\mathcal{X}\| \leq \sqrt{n}$, therefore, the previous statement can be restated in our final form as: there exists a matrix $\Delta \in \mathbb{R}^{n,n}$ in the set $\{\Delta : \|\Delta\| \leq 1\}$, such that $\mathcal{R} = L\Delta$, with

$$L = \frac{\sqrt{n}}{2} \|E\| \text{diag}(m_1, \dots, m_n).$$

From this follows that the expansion (18) can always be written in the form

$$f(x) = f(\hat{x}) + (A + L\Delta)(x_k - \hat{x}_k)$$

for some value of Δ with $\|\Delta\| \leq 1$.

REFERENCES

- [1] T. W. Anderson, *An Introduction to Multivariate Statistical Analysis*. New York: Wiley, 1958.
- [2] B. Anderson and J. B. Moore, *Optimal Filtering*. Englewood Cliffs, NJ: Prentice-Hall, 1979.
- [3] D. P. Bertsekas and I. B. Rhodes, "Recursive state estimation for a set-membership description of uncertainty," *IEEE Trans. Autom. Control*, vol. 16, no. 2, pp. 117–128, Feb. 1971.
- [4] M. Betke and L. Gurvits, "Mobile robot localization using landmarks," *IEEE Trans. Robot. Autom.*, vol. 13, no. 2, pp. 251–263, Feb. 1997.

- [5] S. Boyd, L. El Ghaoui, E. Feron, and V. Balakrishnan, "Linear matrix inequalities in system and control theory," in *Studies in Applied Mathematics*. Philadelphia, PA: SIAM, 1994.
- [6] G. Calafiore and L. El Ghaoui, "Ellipsoidal bounds for uncertain linear equations and dynamical systems," *Automatica*, vol. 50, no. 5, pp. 773–787, 2004.
- [7] F. Dellaert, D. Fox, W. Burgard, and S. Thrun, "Monte Carlo localization for mobile robots," in *Proc. IEEE Int. Conf. Robot. Autom.*, Detroit, MI, May 1999, pp. 1322–1328.
- [8] L. El Ghaoui and G. Calafiore, "Robust filtering for discrete-time systems with bounded noise and parametric uncertainty," *IEEE Trans. Autom. Control*, vol. 46, no. 7, pp. 1084–1089, Jul. 2001.
- [9] L. El Ghaoui and J.-L. Commeau, (1999, January) `lmitool` Version 2.0. [Online] Available: <http://www.ensta.fr/~gropco>
- [10] G. A. Einicke and B. White, "Robust extended Kalman filtering," *IEEE Trans. Signal Process.*, vol. 47, no. 9, pp. 2596–2599, Sep. 1999.
- [11] E. Fabrizi, G. Oriolo, S. Panzneri, and G. Ulivi, "A KF-based localization algorithm for nonholonomic mobile robots," in *Proc. 6th IEEE Mediterranean Conf.*, Alghero, Italy, Jun. 1998, pp. 130–135.
- [12] L. Jetto, S. Longhi, and G. Venturini, "Development and experimental validation of an adaptive extended Kalman filter for the localization of mobile robots," *IEEE Trans. Robot. Autom.*, vol. 15, no. 2, pp. 219–229, Apr. 1999.
- [13] M. Kieffer, L. Jaulin, E. Walter, and D. Meizel, "Robust autonomous robot localization using interval analysis," *Reliable Comput.*, vol. 6, no. 3, pp. 337–362, 2000.
- [14] J. J. Leonard and H. F. Durrant-Whyte, *Directed Sonar Sensing for Mobile Robot Navigation*. Boston, MA: Kluwer, 1992.
- [15] A. Kurzhanski and I. Vályi, *Ellipsoidal Calculus for Estimation and Control*. Boston, MA: Birkhäuser, 1997.
- [16] R. Mandelbaum and M. Mintz, "A confidence set approach to mobile robot localization," in *Proc. IEEE/RSJ Int. Conf. Intell. Robots Syst.*, Osaka, Japan, 1996, pp. 481–488.
- [17] R. M. Murray and S. S. Sastry, "Nonholonomic motion planning: steering using sinusoids," *IEEE Trans. Autom. Control*, vol. 38, no. 5, pp. 700–716, May 1993.
- [18] S. S. Qing-Hao-Meng, S. S. Yi-Cai-Sun, and S. S. Zuo-Liang-Cao, "Adaptive extended Kalman filter (AEKF)-based mobile robot localization using sonar," *Robotica*, vol. 18, no. 5, pp. 459–473, 2000.
- [19] S. I. Roumeliotis and G. A. Bekey, "Bayesian estimation and Kalman filtering: a unified framework for mobile robot localization," in *Proc. IEEE Int. Conf. Robot Autom.*, San Francisco, CA, Apr. 2000, pp. 2985–2992.
- [20] K. T. Sutherland and W. B. Thompson, "Localizing in unstructured environments: dealing with the errors," *IEEE Trans. Robot. Autom.*, vol. 10, no. 6, pp. 740–754, Jun. 1994.
- [21] L. Vandenberghe and S. Boyd, "Semidefinite programming," *SIAM Rev.*, vol. 38, no. 1, pp. 49–95, 1996.



Giuseppe Calafiore received the Laurea degree in electrical engineering and the Ph.D. degree from Politecnico di Torino, Torino, Italy, in 1993 and 1997, respectively.

Since 1998, he has held the tenured position of Assistant Professor with the Dipartimento di Automatica e Informatica, Politecnico di Torino. He has held visiting positions in the Information Systems Laboratory, Stanford University, Stanford, CA, in 1995, at the Ecole Nationale Supérieure de Techniques Avancées (ENSTA), Paris, France, in 1998, and at the University of California (UC), Berkeley, in 1999. In 2003, he was a Research Engineer in the Electrical Engineering and Computer Science Department, UC Berkeley. He is the author of over 60 technical papers and three books. His research interests are in the fields of convex optimization, randomized algorithms, robotics, and the analysis and control of uncertain systems.